

## Valence-band electronic structure of silicon nitride studied with the use of soft-x-ray emission

R. D. Carson and S. E. Schnatterly

*Jesse Beams Laboratory of Physics, University of Virginia, Charlottesville, Virginia 22901*

(Received 29 July 1985)

We have studied the valence-band electronic structure of  $\alpha$ -phase,  $\beta$ -phase, and amorphous silicon nitride samples, using Si  $L$ -x-ray emission. Our results are compared with a recent band-structure calculation and show that Si  $3d$  states are necessary to properly describe the upper-valence-band and lower-conduction-band density of states. A prominent feature is seen above the valence band which is attributed to conduction-band states that are populated by the incident electron beam. By reducing the energy of the electron beam it is possible to enhance the surface emission relative to bulk emission, and such spectra are also presented and discussed.

### I. INTRODUCTION

In recent years soft-x-ray emission (SXE) has been used to study the valence-band density of states (DOS) of many materials. Soft-x-ray emission is complementary to the photoelectron spectroscopic techniques [x-ray photoemission spectroscopy (XPS), ultraviolet photoemission spectroscopy (UPS)] which are useful primarily near the surface. While SXE is used mainly for bulk studies (1000–2000 Å penetration), it is possible to enhance the surface sensitivity by reducing the energy of the incident electrons used to excite the x rays. Although there has been some previous experimental work on silicon nitride using SXE (Refs. 1 and 2) and XPS (Ref. 3) only amorphous films have been studied, and there appears to be no previous surface-enhanced SXE work in the literature. Using Si  $L_{II,III}$ -x-ray emission we have studied the valence-band electronic structure of  $\alpha$ -phase and  $\beta$ -phase crystalline and thin-film amorphous silicon nitride samples. The amorphous sample was also studied at reduced incident electron energy to emphasize the surface.

There have been recent electronic structure calculations on silicon nitride. Sokel<sup>4</sup> performed a linear combination of atomic orbital (LCAO) calculation assuming silicon  $sp^3$  hybrid states and nitrogen  $2s, 2p$  states; in this model the effect of the Si–N–Si bond angle on the electronic states was considered. Robertson<sup>5</sup> performed a calculation using a bond-orbital model and assumed two different values for the Si–N–Si bond angle; the electronic structure of several likely impurities was considered and it was found that some resulted in band-gap states. Ren and Ching<sup>6</sup> performed a calculation using an orthogonalized LCAO model; their calculation was performed on  $\alpha$ - and  $\beta$ -phase crystalline silicon nitride and was done with and without Si  $3d$  states included in the basis set. We will compare our silicon nitride SXE spectra to the calculated DOS of Ren and Ching.

### II. EXPERIMENT

The data presented in this paper were taken on a soft-x-ray spectrograph which covers the energy range 20–800 eV. The electron gun used to excite the x rays produces

currents of about a milliamper and the incident kinetic energy could be varied over the range 300 to 3000 eV; at low kinetic energy the surface emission is considerably enhanced. The dispersive elements are four toroidal grazing incidence diffraction gratings. The detector is a phosphor-coated photodiode array cooled with liquid nitrogen. Details of the spectrograph have been described previously in the literature.<sup>7,8</sup> For the Si  $L$ -x-ray emission spectra the energy range was 70–110 eV, the resolution was about 0.1 eV, and the calibration uncertainty was about 0.09 eV at 100 eV. During the experiment the sample chamber was maintained as a pressure of  $10^{-8}$  Torr or better. An argon ion gun mounted in the sample chamber was used to clean the samples if necessary.

The  $\alpha$ -phase and  $\beta$ -phase crystalline samples were made from commercially available micrometer-size powders. The powders were pressed into a copper substrate which had been wet with indium. The amorphous sample was a thin film approximately 1000 Å thick grown on a silicon substrate by chemical vapor deposition (CVD). The amorphous samples also had transmission windows covered only by the 1000-Å CVD film and could be studied in a related inelastic electron scattering experiment; this allowed the determination of the x-ray absorption coefficient of the CVD films in the energy range studied by the SXE experiment.

### III. DATA PROCESSING

The unprocessed spectra are functions of several energy-dependent factors in addition to the desired features in the electronic structure. These include instrumental effects, self-absorption, various background contributions, and the radiative transition probability. These various effects can be summarized by the following relation in which  $I(E)$  represents the unprocessed spectral intensity:

$$I(E) \sim \{[D(E)P(E) + B(E)]A(E) + M(E)\}S(E),$$

where  $S(E)$  is the spectrometer response,  $M(E)$  the multiple-order interference,  $A(E)$  the self-absorption factor,  $B(E)$  the background contributions,  $P(E)$  the radia-

tive transition probability, and  $D(E)$  the transition density. Proceeding from right to left in the above equation the first two terms  $S(E)$  and  $M(E)$  are both instrumental in origin.  $S(E)$  represents the energy-dependent spectrometer response due to grating dispersion and the detector phosphor efficiency; the correction due to the spectrometer response must be applied to any spectrum.  $M(E)$  represents the interference, if present, from a higher-energy emission appearing in multiple order in the desired first-order spectrum. This is the case in the Si  $L$  emission spectrum of silicon nitride. The nitrogen  $K$  emission occurs at about 396 eV and appears in fourth order at 99 eV where it interferes with the first-order Si  $L$  emission. However, by measuring the nitrogen  $K$  emission of silicon nitride in third order at 132 eV and then scaling the energy values by  $\frac{3}{4}$  a good measure of  $M(E)$  is obtained and this can then be removed from the Si  $L$  spectrum. In the case of silicon nitride the spectrum can be severely distorted if there is instrumental interference from fourth order  $N$  and this appears to have occurred in the earlier work.<sup>1,2</sup> If the fourth order  $N$  is not removed the feature at the top of the valence band is too intense.

Next the measured spectra are corrected for self-absorption. The self-absorption factor  $A(E)$  depends on the depth from which the x rays are emitted as well as the energy-dependent x-ray absorption coefficient  $\alpha(E)$ . Assuming that each layer of sample down to the maximum x-ray escape depth  $X_{\max}$  radiates x rays equally, the self-absorption for all layers  $A(E)$  is found by simple integration to be

$$A(E) = \left( \frac{1 - e^{-\alpha X_{\max}}}{\alpha X_{\max}} \right).$$

The x-ray escape depth is approximately twice the electron penetration depth for flat samples mounted at about a 30° angle to the horizontal plane of the spectrograph. This was the case for the CVD film amorphous samples and resulted in a maximum escape depth estimate of  $X_{\max} \approx 1600$  Å. However, in the case of the  $\alpha$ -phase and  $\beta$ -phase material the samples were micrometer-size powders. Therefore one would expect a distribution of angles which the faces of the powder particles make with the horizontal. In this case it was assumed that the average x-ray escape depth was equal to 1600 Å just as in the CVD sample. As previously mentioned, the absorption coefficient  $\alpha(E)$  was determined for the CVD film sample in an auxiliary inelastic electron spectroscopy experiment. The x-ray absorption measurements for the CVD film samples were used for self-absorption corrections on all three samples since absorption data for the  $\alpha$ -phase and  $\beta$ -phase crystalline samples were not available. For these reasons the self-absorption correction may not be quite correct for the  $\alpha$ -phase and  $\beta$ -phase spectra. An empirical range formula<sup>9</sup> developed for use over the energy range 1–10 keV was used to estimate the electron penetration at 3 keV. This formula is of the form  $R = bE^n$ , where  $R$  is the range in angstroms and  $E$  is the electron kinetic energy in keV; the constants  $b$  and  $n$  are dependent on the material properties such as density, molecular weight, and the number of electrons per atom. The range formula

predicts a penetration for silicon nitride of about 800 Å at 3 keV. However, at 500 eV the formula predicts about 10 Å which is not realistic. A more reasonable estimate of the penetration at 500 V can be obtained by assuming the electron to follow a random walk as it makes a succession of inelastic collisions. A reasonable estimate of the inelastic mean free path is about 10–15 Å and the average energy loss per collision about 20–25 eV. Thus a 500-eV electron would make about 20–25 collisions and the square root of this number (4–5 mean free paths) would apply toward progress in a given direction for the random walk. This results in an estimated penetration of 50–60 Å. Of course in the case of Si  $L$ -x-ray emission the quantity of interest is the maximum depth at which  $2p$  core holes are still found; this depth is certainly less than a range estimate since once the electron energy falls below 100 eV it cannot create  $2p$  core holes.

In general a number of sources contribute to the energy-dependent background  $B(E)$ . These include bremsstrahlung x-ray intensity, emission from radiative Auger processes,<sup>10,11</sup> plasmon low-energy satellites, and double-core-vacancy high-energy satellites. For the data being presented here only the bremsstrahlung x-ray contribution is significant. The featureless bremsstrahlung spectrum is considered linear over the limits of the valence band; the slope is determined by the measured intensity at each end of the spectrum (70 and 110 eV).

In the dipole approximation x-ray emission is proportional to a dipole matrix element, a radiative transition probability  $P(E)$ , and the valence-band transition density  $D(E)$ . The dipole matrix element results in the usual selection rules and is assumed independent of energy over the valence band.  $P(E)$  is proportional to  $E^3$  and this must be divided out to finally recover  $D(E)$ . Within the one-electron approximation  $D(E)$  is then proportional to a projection of the usual density of states for the valence band in question. In the data presented in this paper the  $D(E)$  curves have been normalized to an area of unity so that the vertical axes have units of states per eV.

#### IV. RESULTS AND DISCUSSION

First we will briefly discuss the results of the calculated DOS of Ren and Ching comparing their results obtained with and without the presence of Si  $3d$  states. Then our bulk spectrum of  $\beta$ -Si<sub>3</sub>N<sub>4</sub> will be compared with these calculated DOS. Finally our spectra for the  $\alpha$ -phase,  $\beta$ -phase, and CVD amorphous Si<sub>3</sub>N<sub>4</sub> are compared with each other. Comparisons will also be made between spectra taken with 3-keV electron beams (bulk) and those taken with 500-V beams (surface) for the  $\beta$ -phase and CVD samples.

The calculation of Ren and Ching was performed using orthogonalized linear combinations of atomic orbitals (OLCAO) in which the valence orbitals were made orthogonal to core states. This was applied to the  $\alpha$ -phase and  $\beta$ -phase crystalline silicon nitride structures using the crystal atom positions and free-atom Hartree-Fock wave functions as input. This allowed the atomic potentials to be calculated using an overlap of atomic charge density model. Gaussian-type orbitals (GTO) were used as basis

functions to solve the eigenvalue problem for each atom.

The results of these band-structure calculations for  $\beta$ - $\text{Si}_3\text{N}_4$  are shown in Fig. 1. In Fig. 1(a) is shown the Si DOS calculated using a "minimal basis" set without Si 3*d* states (1*s*, 2*s*, 2*p*, 3*s*, 3*p*). When Si 3*d* states were added to this minimal basis set the results in Fig. 1(b) were obtained. Figure 1(c) was calculated with an "extended basis" set. The extended basis set also used Si 3*d* states but in addition included two extra *s*-type and one extra *p*-type GTO functions for both the Si and N atoms. As is evident from the figure the main effect of including the 3*d* states is to put strength into the upper valence band and lower conduction band. Note in particular that the feature at the top of the valence band is nearly gone when the minimal basis is used [Fig. 1(a)]. Thus the Si 3*d* states appear to be necessary to provide intensity in the upper 2 V of the Si valence-band DOS. A similar situation has been noted for the case of silicon dioxide.<sup>12,13</sup>

A comparison between the calculated DOS using the extended basis and our measured spectra for  $\beta$ - $\text{Si}_3\text{N}_4$  is shown in Fig. 2. The energy axis has been shifted so that there is optimal agreement between the measured spectrum and the calculated DOS. The main features have been labeled *A*, *B*, *C*, *D*, and *E* in order of increasing energy. Feature *A* at about 81 eV results from the effect that the N 2*s* orbitals have on the Si DOS. The molecular-orbital  $\sigma$  bonds between Si  $sp^3$  hybrid orbitals and N  $sp^2$  hybrid orbitals produce a strong peak in the Si spectra at 90 eV (feature *B*). There is a very strong peak in the N partial DOS just below the top of the valence band which comes from the N lone-pair 2*p* electrons; also at the top of the valence band in the Si DOS is a feature which only appears when the Si 3*d* orbitals are used [Figs.

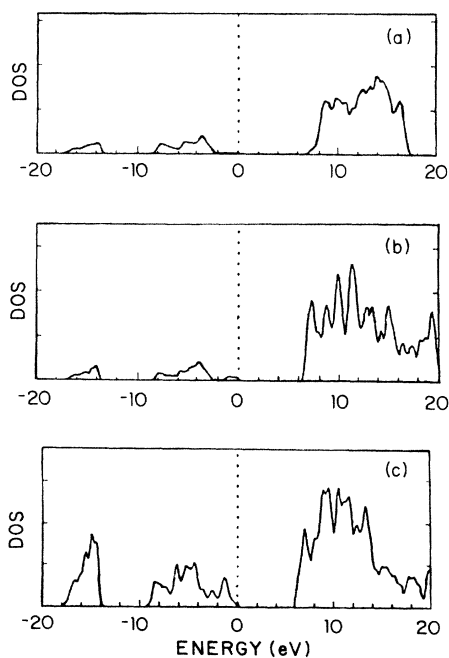


FIG. 1. Calculated silicon DOS for  $\beta$ -phase silicon nitride according to Ren and Ching. Zero of energy is at the top of the valence band. (a) Minimal basis calculation; (b) using 3*d* states; (c) extended basis states.

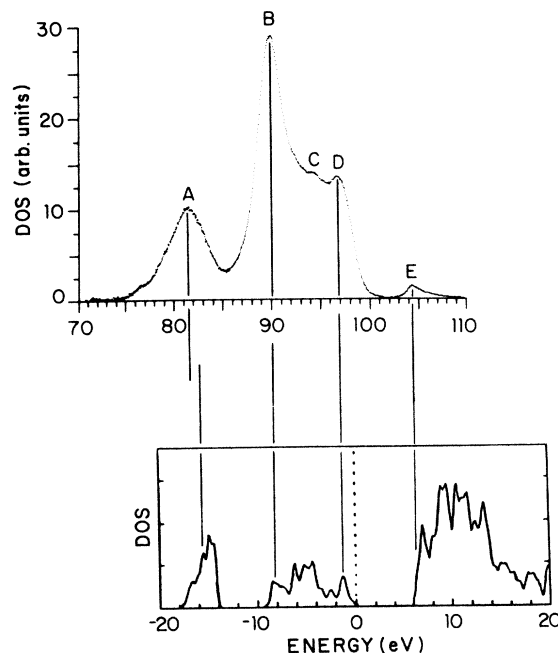


FIG. 2. Comparison of experimental and calculated (extended basis) DOS for  $\beta$ -phase silicon nitride. Energy scales have been shifted to produce optimal agreement of the features.

1(b) and 1(c)]. This suggests that some degree of  $p\pi$  molecular-orbital bonding occurs between N lone-pair 2*p* states and normally empty Si 3*d* states as has been suggested.<sup>14</sup> Feature *D* is thus assigned to Si 3*d* states. We believe that the structure at 104 eV (feature *E*) represents electron states in the lower conduction band which have been populated by the incident electron beam. Note that features *B*, *D*, and *E* align well with the calculated Si DOS when the top of the valence band ( $E=0$ ) is placed at about 98 eV in the spectrum. There is a 1–2-eV discrepancy between the measured spectra and calculated DOS for feature *A*. This discrepancy was also noted by Ren and Ching when they compared their calculated DOS to the experimental XPS spectra of Weinberg and Pollack.<sup>3</sup>

The origin of feature *C* is unclear. To our knowledge this feature has not been previously reported in earlier SXE measurements. Two possible extraneous explanations of the feature are third-order *K* emission from carbon contamination or *L* emission from  $\text{SiO}_2$  contamination. Feature *C* is located at about 94.3 eV, third-order carbon at 92.0 eV, and the upper valence-band feature of  $\text{SiO}_2$  at 94.5 eV. Third-order carbon must be ruled out since it is too far removed in energy. Although  $\text{SiO}_2$  emission could be the source it is difficult to accept this as the explanation. Feature *C* is just as prominent in  $\alpha$ -phase and  $\beta$ -phase crystalline samples as in the CVD sample, yet the crystalline samples should be rather pure and free of oxygen. Indeed when the O *K* emission and N *K* emission were compared in each sample it was estimated that less than 1% of the N atoms had been replaced by O atoms, so we do not believe that this is the origin of the feature. A third possibility is that *C* is a real feature in the valence-band DOS resulting from Si 3*p* states. This

TABLE I. Listed are the measured energies (eV) for features  $A-E$  of the bulk and surface data. The N  $2S$  and exciton areas are expressed as a fraction of the total spectral area. The fit parameters ( $E_v, \sigma_v, \sigma_c$ ) are shown at the right and are in eV. The extrapolated band edge is listed as  $E'_v$ .

Sample	$A$	$B$	$C$	$D$	$E$	N $2S$ area	Exciton area	$E'_v$	$E_v$	$\sigma_v$	$\sigma_c$
Bulk											
$\alpha$	81.5	90.0	94.3	96.7	104.3	0.21	0.020	99.6	98.7	0.9	0.7
$\beta$	81.5	89.9	94.5	96.6	104.3	0.21	0.016	99.4	98.5	1.0	0.6
CVD	81.4	89.8	94.0	96.7	104.2	0.25	0.0082	99.4	98.8	0.8	0.5
Near surface											
$\beta$	81.4	89.9	?	96.6	104.0	0.15	0.0045	99.4	98.3	1.2	0.5
CVD	81.3	90.0	94.0	96.6	104.2	0.23	0.011	99.4	98.9	0.8	1.0

cannot be ruled out by dipole selection rules if the  $3p$  state and the  $2p$  core hole are associated with different  $\text{Si}$  atoms. The Si-Si nearest-neighbor separation is about 3 Å in  $\beta\text{-Si}_3\text{N}_4$ . Using Hermann-Skillman wave functions<sup>15</sup> for the Si  $2p, 3s$  states and nearest-neighbor Si  $3p$  states a rough estimate of the matrix elements suggests that the probability of making such a nearest-neighbor transition is about 5–10% of the probability of a one-atom ( $3s \rightarrow 2p$ ) transition. Thus it is reasonable that small features in the spectrum could be due to such transitions. This interpretation is consistent with the results reported by Brytov *et al.*<sup>2</sup> in which the Si  $K$ - and  $L$ -x-ray spectra were compared. When the  $K$  and  $L$  spectra were aligned in energy the main peak in the  $K$  spectrum from  $3p$  states corresponded to 94.5 eV in the  $L$  spectrum. Although the  $L$  spectrum of Brytov does not clearly show a feature at this energy, our feature  $C$  lies within 0.2 eV of this point.

When the spectra of  $\alpha$ -phase,  $\beta$ -phase, and CVD samples are compared they appear quite similar, unlike the case of elemental silicon in which there are marked differences between the crystalline and amorphous spectra. The spectrum of each sample is shown in Fig. 3. Table I shows the approximate energy of the spectral features in each sample. Also shown for each sample is an estimate of the upper valence-band edge ( $E_v$ ), the broadening of this edge ( $\sigma_v$ ), and the width of the conduction-band peak ( $\sigma_c$ ). The valence-band edge was assumed to be linear in energy and broadened by a Gaussian and the conduction-band peak was assumed to be a Gaussian. The major difference is in the intensity of feature  $A$  in the CVD spectrum—it is considerably more intense than in the  $\alpha$ -phase and  $\beta$ -phase samples. The fractional area of feature  $A$  was measured for the  $\alpha$ -phase,  $\beta$ -phase, and CVD samples and found to be 0.21, 0.21, and 0.25, respectively.

In order to facilitate comparisons the difference between each pair of spectra has been plotted in Fig. 4. As can be seen from the figure the  $\alpha$  phase and  $\beta$  phase are the most similar. The strength of feature  $A$  in the CVD spectrum is responsible for the pronounced dip at 82 eV in the difference plots. Notice the region between 85 and 95 eV in each difference spectrum. For the  $\alpha$ -CVD and  $\beta$ -CVD plots the shape in this region indicates that both the  $\alpha$  and  $\beta$  spectra have a broader  $B$  feature than does the CVD spectrum. The shape of the  $\alpha$ - $\beta$  plot suggests that feature  $B$  of the  $\alpha$ -phase spectrum is shifted upward relative to the  $\beta$ -phase spectrum. Table I shows this shift

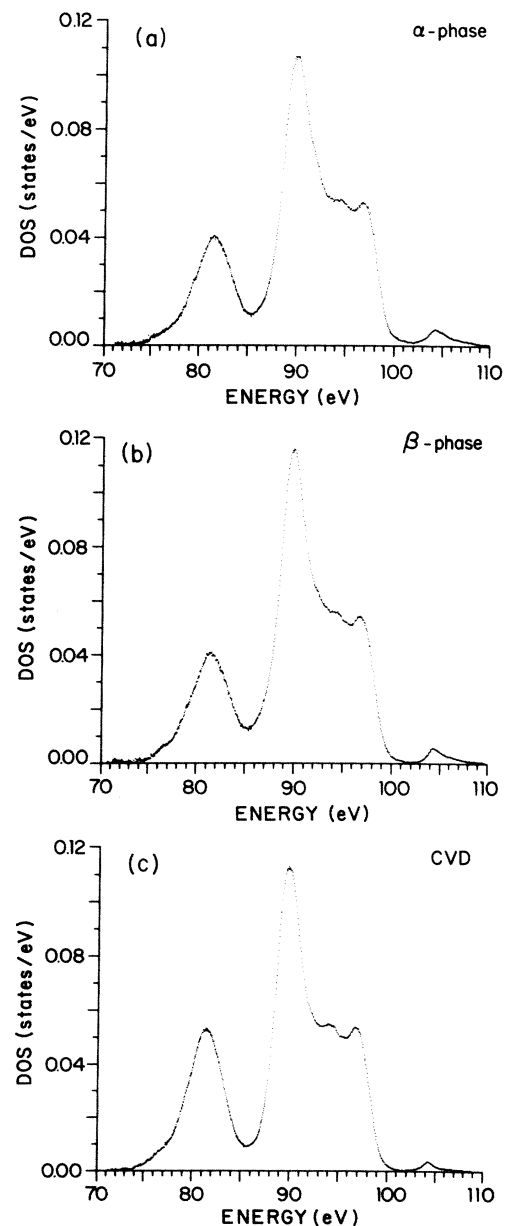


FIG. 3. Experimentally measured bulk DOS for silicon nitride samples. Data have been normalized so that the area under each curve corresponds to one electron state. Horizontal scales are in eV.

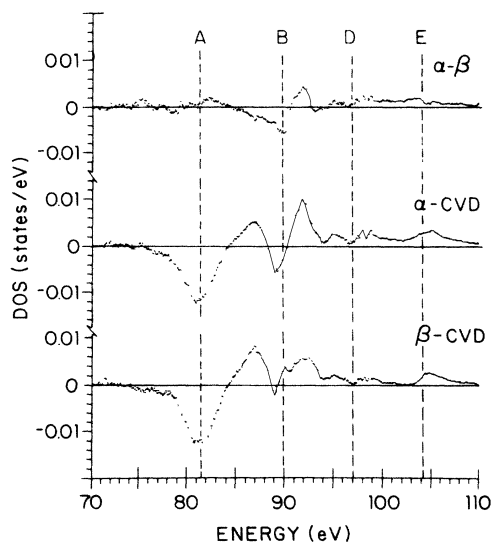


FIG. 4. Difference curves for bulk silicon nitride spectra of Fig. 3. Dashed vertical lines indicate position of features in Fig. 2.

to be about 0.1 eV. There are also differences which appear in the region above the valence band (100–105 eV). The exciton in the  $\alpha$ -phase sample is stronger but broader than in either of the other two samples. In fact all of the features of the  $\alpha$ -phase spectrum appear broadened when compared to the other two samples; this is most evident in the features *B* and *E*. It is reasonable that the  $\alpha$ -phase spectrum should show increased broadening compared to the  $\beta$  phase since the  $\alpha$ -phase unit cell is more complex. The  $\alpha$ -phase unit cell has 12 Si atoms while the  $\beta$  phase only has 6 Si atoms.<sup>16</sup> This means that  $\alpha$  phase has more inequivalent site Si atoms which may explain the increased broadening. It is rather surprising, however, that the CVD spectrum appears to be the sharpest of the three spectra.

Since peak *A* is associated with N 2s states, changes in stoichiometry might affect its intensity. As a rough estimate of the stoichiometry the ratio of third-order N *K* emission (132 eV) to the Si *L* emission (90 eV) was measured for both the  $\beta$ -phase and CVD samples. It was found that this ratio was 0.067 for the  $\beta$  phase and 0.061 for the CVD sample; the uncertainty in these ratios is about 5%. Thus the CVD sample appears to have a slight deficit in N suggesting a weaker peak-*A* intensity. We therefore conclude that the observed peak-*A* differences are not due to stoichiometry but instead to structural differences between crystalline and CVD amorphous silicon nitride.

#### A. Near-surface emission

Surface spectra for both  $\beta$ -phase and CVD samples have been taken and have been compared with the bulk spectra. The surface spectra were taken using 500-V incident electron energies with an assumed electron penetration of about 50 Å whereas the bulk spectra used 3-kV electrons with a 800-Å penetration depth. Figure 5 shows the surface spectra and Fig. 6 shows the bulk-surface

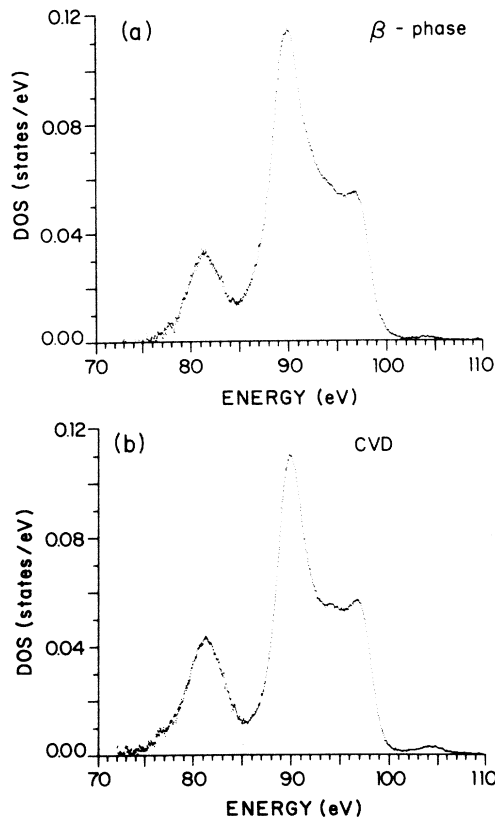


FIG. 5. Experimentally measured near-surface DOS for  $\beta$ -phase crystalline and amorphous CVD film silicon nitride. Data have been normalized so that the area under each curve corresponds to our electron state. Horizontal scales are in eV.

difference spectrum for each sample. The surface spectra show increased broadening and have differences in the band gap and exciton region when compared with the bulk spectra. The surface broadening appears greater in the  $\beta$ -phase sample than in the CVD film sample. Note

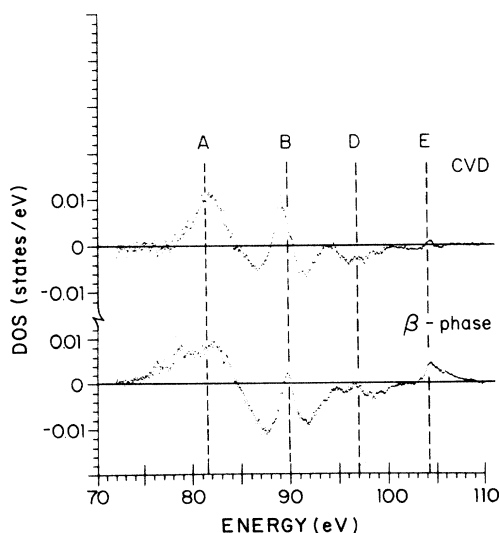


FIG. 6. Difference curves for near-surface silicon nitride spectra of Fig. 5. Dashed vertical lines indicate position of features in Fig. 2.

that in the  $\beta$ -phase surface spectrum feature *C* cannot be resolved. Also, feature *B* in the CVD surface spectrum seems to be shifted to higher energy by about 0.2 eV; this is evident in the CVD bulk-surface difference plot which shows a derivative shape, near peak *B*. This shift is also noted in the data in Table I. In both the  $\beta$ -phase and CVD surface spectra feature *A* appears weaker as can be seen by the positive difference values between 75–85 eV.

There are two reasons why surface broadening may be occurring. First there could be a surface core-level shift; such a shift could be important in our surface data where the estimated electron penetration is only about 50 Å. Such core-level shifts have been reported in the case of crystalline Si and Au (Refs. 17 and 18) and were in the direction of weaker core-level binding at the surface. In both cases these shifts are in the wrong direction to explain our data in which peak *B* is asymmetrically broadened toward higher energies in the surface spectra.

It is also possible that the surface spectra reflect a different DOS. A number of workers in recent years have dealt with DOS changes at the surface due to dangling bonds, relaxation, or rehybridization.<sup>19,20</sup> In the case of crystalline Si it has been shown that surface states produce two new bands in the valence band as well as states in the band gap.<sup>19</sup> It is known that when surface rehybridization occurs (e.g.,  $sp^3$  to  $sp^2$ ) that bond lengths are often shortened. It might be reasonable that this would promote increased interaction among surface atoms and thus broaden the electronic structure.

### B. Gap region and exciton

The region above the valence band in silicon nitride displays a rather pronounced feature at about 104 eV (feature *E*). Structure such as this is not uncommon in large-band-gap materials and can in part be attributed to self-absorption. Zhukova *et al.*<sup>1</sup> explained it as bremsstrahlung x-ray intensity with self-absorption which began at 104 eV. However, when our silicon nitride spectra were corrected for self-absorption as previously discussed, it was found that the feature at *E* remained although the gap region intensity was considerably reduced. Brytov *et al.*<sup>2</sup> measured a feature at about 103 eV and explained it as emission from a state in the band gap; our measurements do not agree with this energy. As shown in Fig. 2 feature *E* aligns well with the bottom of the conduction band in the calculated DOS. We identify the feature at 104 eV as a Si core exciton because its energy agrees with our measured Si  $2p$  core threshold (104.0 eV at the 50% point) in absorption using inelastic electron scattering. Using our measured values of the valence-band edge and conduction-band exciton the apparent band gap is about 5.5 eV. Measurements on silicon nitride using optical techniques give values for the band gap which range between 5.1 and 5.3 eV.<sup>21–23</sup>

Although Table I shows that our fits suggest a band gap of 5.5–5.8 eV this is probably too large. When the top of the valence band was fit as described above, a broadening of the valence band,  $\sigma_v$ , was determined which we believe to be excessive. Note that the valence-band

broadening is usually considerably larger than the conduction-band broadening. This could be the result of gap states just above the valence band which have not been included in the fitting function and would require a larger  $\sigma_v$ . The interplay between  $\sigma_v$  and  $E_v$  is such that increasing  $\sigma_v$  tends to reduce  $E_v$  and this is probably responsible for the large band gap. It is likely that the broadening for both valence and conduction band is approximately 0.5–0.7 eV exclusive of gap states and that gap states are responsible for part of the valence-band tail. When a simple linear extrapolation is applied to the data near the top of the valence band, values for the edge of about 99.3–99.5 eV are obtained which gives a band gap of 4.7–4.9 eV. This leaves room for a small exciton shift which should be reasonable.

What is unusual about silicon nitride is the intensity of this core exciton when compared with other large-band-gap materials. For example, when silicon dioxide is studied using SXE the core exciton is very weak or absent. Both silicon nitride and silicon dioxide have much greater strength of the Si DOS in the conduction band than in the valence band yet only silicon nitride shows a strong core exciton. Why this is so is not clear but it is probably due to an efficient mechanism for electron trapping peculiar to silicon nitride. Electron trapping in silicon nitride has been studied extensively because of its application in memory devices. In studies of capacitors in which silicon nitride was the dielectric it has been determined that electron trapping extends into the bulk with trapped electron densities measured at  $6 \times 10^{18}$  e/cc;<sup>24</sup> it was noted that the trap density could have been much higher than this value.

Knowing the area under the exciton peak allows a rough estimate of the trapped electron concentration associated with the exciton as seen in our SXE experiment. The area under the valence band is about 1 and the exciton peaks had areas of 0.005–0.02. Assuming that one electron per silicon atom contributes to the valence-band emission, simple rate-equation arguments suggest that the minimum lifetime for trapped electrons must be at least  $10^{-7}$  sec to account for this 1% exciton strength. This represents a lower limit to the trap lifetime. Traps present in the sample but not created by the incident electron beam could have a longer lifetime and still contribute to the emission we see.

The bulk spectra of all three samples appeared to show emission in the band-gap region even after correcting for self-absorption. The gap emission of the CVD sample was much closer to the background level and this may reflect a better self-absorption correction for the CVD sample. As seen in Fig. 3 there appears to be considerable intensity in the band gap due only to the broadening of the valence-band edge and exciton. Because of this and the uncertainty in the self-absorption correction, particularly in the crystalline samples, it is not possible to say with certainty that there is band-gap emission. A stronger case can be made for gap emission when the CVD near-surface emission is examined. As shown in Fig. 5 there is definite evidence for the emission from gap states near the surface. The assumed x-ray escape depth was 100 Å for the 500-V spectra. To make the intensity between 100 and 104 eV

approach the background level an unrealistic x-ray escape depth far in excess of 100 Å would be necessary. Therefore it is assumed that this emission is from gap states predominately at the surface. Such band-gap emission could result from damaged structure, dangling bonds, or impurities which might be present in higher concentration near the surface. Robertson<sup>5</sup> has investigated various impurity configurations in silicon nitride and shown that some result in gap states which are not removed by hydrogenation.

## V. CONCLUSIONS

Several conclusions can be made based on our SXE study of the silicon nitride samples. These are listed below.

(1) Bulk SXE qualitatively agrees with the calculated DOS provided Si 3*d* states are used in the calculation. The 3*d* states are required for the proper structure in the upper valence band and lower conduction band.

(2) The feature above the valence band at 104 eV is not due to self-absorption or band-gap states but is the result of lower conduction-band states which are populated by the electron beam forming a core exciton.

(3) The feature in the middle of the valence band (feature C) is the result of transitions between Si 3*p* valence states and nearest-neighbor Si 2*p* core states. This

is somewhat unusual in that Si *L* spectra are generally considered to reveal only *s* and *d* valence states.

(4) The  $\alpha$ ,  $\beta$ , and CVD spectra are all very similar with the closest agreement being between the  $\alpha$ -phase and  $\beta$ -phase crystalline samples. The CVD result differs from the crystalline in two respects—the CVD spectrum is somewhat sharper and it has a stronger low-energy feature; the strength of this feature is probably not the result of altered stoichiometry but reflects a different Si DOS for the CVD sample.

(5) For both  $\beta$ -phase and CVD samples the surface data differ from bulk data in three respects.

(a) The surface spectra are broadened.

(b) The surface spectra have weaker low-energy peaks.

(c) The surface spectra have weaker excitons and may have surface gap states.

## ACKNOWLEDGMENTS

We wish to thank J. Nithianandam for assistance in sample preparation. We also wish to recognize the other members of our group, P. Bruhwiler, A. Cafolla, D. Husk, P. Livins, A. Mansour and C. Tarrío, for their helpful suggestions and discussions throughout the course of this work. This work was supported in part by National Science Foundation Grant No. DMR-82-14968.

<sup>1</sup>I. I. Zhukova *et al.*, *Fiz. Tverd. Tela* (Leningrad) **10**, 1383 (1968) [*Sov. Phys.—Solid State* **10**, 1097 (1968)].  
<sup>2</sup>I. A. Brytov *et al.*, *Fiz. Tverd. Tela* (Leningrad) **26**, 1685 (1984) [*Sov. Phys.—Solid State* **26**, 1022 (1984)].  
<sup>3</sup>Z. A. Weinberg and R. A. Pollak, *Appl. Phys. Lett.* **27**, 254 (1975).  
<sup>4</sup>R. J. Sokel, *J. Phys. Chem. Solids* **41**, 899 (1980).  
<sup>5</sup>J. Robertson, *Philos. Mag. B* **44**, 215 (1981).  
<sup>6</sup>S. Y. Ren and W. Y. Ching, *Phys. Rev. B* **23**, 5454 (1981).  
<sup>7</sup>(a) T. Aton *et al.*, *Nucl. Instrum. Methods* **172**, 173 (1980); (b) F. Zutavern *et al.*, *Nucl. Instrum. Methods* **172**, 351 (1980).  
<sup>8</sup>R. D. Carson *et al.*, *Rev. Sci. Instrum.* **55**, 1973 (1984).  
<sup>9</sup>C. Feldman, *Phys. Rev.* **117**, 455 (1960).  
<sup>10</sup>J. Pirenne and P. Longe, *Physica* **30**, 277 (1964).  
<sup>11</sup>P. Livins and S. E. Schnatterly (unpublished).  
<sup>12</sup>Collins *et al.*, *J. Chem. Soc. Faraday Trans. II* **68**, 1189 (1972).  
<sup>13</sup>W. Beall Fowler, *J. Phys. Chem. Solids* **42**, 623 (1981).  
<sup>14</sup>P. E. D. Morgan, U. S. Office of Naval Research (Arlington,

VA) Report No. F-C2429-06 (unpublished); also in *Nitrogen Ceramics*, edited by F. Riley (Nordhoff, Leyden, 1977), p. 23.  
<sup>15</sup>F. Herman and S. Skillman, *Atomic Structure Calculations* (Prentice-Hall, Englewood Cliffs, 1963).  
<sup>16</sup>R. W. G. Wyckoff, *Crystal Structures* (Wiley, New York, 1964), Vol. 2, pp. 157–159.  
<sup>17</sup>P. H. Citrin, and G. K. Wertheim, *Phys. Rev. Lett.* **41**, 1425 (1978).  
<sup>18</sup>F. J. Himpsel *et al.*, *Phys. Rev. Lett.* **45**, 1112 (1980).  
<sup>19</sup>J. S. Applebaum and D. R. Hamann, *Phys. Rev. Lett.* **31**, 106 (1973).  
<sup>20</sup>K. C. Pandey and J. C. Phillips, *Phys. Rev. Lett.* **32**, 1433 (1974).  
<sup>21</sup>J. Bauer, *Phys. Status Solidi A* **39**, 411 (1977).  
<sup>22</sup>A. M. Goodman, *Appl. Phys. Lett.* **13**, 275 (1968).  
<sup>23</sup>D. J. DiMaria and P. C. Arnett, *Appl. Phys. Lett.* **26**, 711 (1975).  
<sup>24</sup>P. C. Arnett and B. H. Yun, *Appl. Phys. Lett.* **26**, 94 (1975); B. H. Yun, *ibid.* **25**, 340 (1974).